ejpmr, 2019,6(1), 291-294

SJIF Impact Factor 4.897

EUROPEAN JOURNAL OF PHARMACEUTICAL AND MEDICAL RESEARCH

www.ejpmr.com

Review Article

ISSN 2394-3211

EJPMR

BRAIN IMAGE SEGMENTATION AND ITS SPECIFIC LOCATION

Sudipta Roy[1] and Samir Kumar Bandyopadhyay*[2]

[1]Institute of Computer Technology (UVPCE), Ganpat University, Ahmadabad, India.
[2]Advisor to Chancellor, JIS University, India.

***Corresponding Author: Dr. Samir Kumar Bandyopadhyay**

Advisor to Chancellor, JIS University, India.

Article Received on 11/11/2018 **Article Revised on 02/12/2018** **Article Accepted on 23/12/2018**

ABSTRACT

The segmentation of brain image abnormalities is the critical task for detecting brain abnormalities. planning appropriate therapy. This paper proposed brain image segmentation, and its location.

KEYWORDS: MRI, Segmentation, K –Means and Tumor.

INTRODUCTION

Automated diagnosis involves image segmentation step which is used to extract the abnormal lesions from brain MRI. The different abnormalities types differ in many computerized aspects such as nature, size, its shape, volume, number and its locations of lesions. The term abnormalities used to generalize the tumor, hemorrhage, and stroke because using automated system classification of different types of abnormalities is very difficult. Brain image segmentation attempts to label pixels by tissue type. Generalized fuzzy c-means algorithm[1-3] uses both pixel attributes and local spatial information that is weighted in correspondence with neighbor elements based on their distance attributes.

A result of the unsupervised segmentation seems to be highly stable, but a comparison with standard unsupervised methods (k-means) is not very significant in the clinical environment as a consequence of the segmentation of multivariate medical images. The color-converted segmentation with Kmeans clustering algorithm[4], and regions of the brain related to hemorrhage can be correctly separated from the colored image and it help pathologist to distinguish lesion size and its region exactly. Its application to several datasets with different abnormality sizes, intensities and locations show that it can automatically detect and segment very different types of brain abnormality with good quality. A symmetric based[5-6] result constitutes the initialization of a segmentation method based on a combination of a deformable model and spatial relations, leading to a precise segmentation of the abnormalities.

Literature Review

Region growing method requires a seed point that is manually selected by the user and removes all pixels connected to the preliminary seed based on some predefined conditions. These conditions can be based on intensity information or boundaries in the image.[7] The possible criterion might be to grow the region until a boundary in the image is met. Region increasing is seldom used alone but usually within a set of image processing operations, mostly for the description of small, simple structures such as tumors or abnormalities and lesions.[8]The manual dealings to obtain the seed point is the significant disadvantage for this region growing. Region growing has also been the restriction to susceptible to noise. These problems may overcome by using a chemotropic region growing algorithm. The technique is not entirely automatic[26], i.e. it requires user interaction for the selection of a seed and secondly the method fails in producing acceptable results in homogeneous areas.

K-nearest Neighbours (KNN) classifier is considered a non-parametric classifier since it makes no underlying assumption about the statistical structure of the data [9]. K-NN only requires an integer k, set of training data and a metric to measure closeness by Euclidean distance. K-NN is easy to implement and debug, in situations where details of the output of the classifier are functional, it can be very effective if some noise reduction techniques have been used to the classifier. k-NN is very sensitive to irrelevant or redundant features because all features contribute to the similarity and thus to the classification and this can be ameliorated by careful feature selection or feature weighting.[10-12]

Proposed Method

The transformation function for RGB image into Gray Scale from input image f(x, y) to processed g(x, y) is given below

$$g(x,y) = T[f(x,y)] \quad (1)$$

T is of size 1×1 (that is, a single pixel) and it is of the form

$$s = T(r)$$

where r and s are variables representing the gray level of f(x, y) and g(x, y) at any point (x, y). Mean is defined as μ.

$$\mu = \frac{1}{MN}\sum_{x=0}^{M-1}\sum_{y=0}^{N-1} f(x,y) \quad (3)$$

Variance is defined as v and its expression is shown below

$$v = \frac{1}{MN}\sum_{x=0}^{M-1}\sum_{y=0}^{N-1}(f(x,y)-\mu)^2 \quad (4)$$

Standard deviation is identified as σ.

$$\sigma = \sqrt{v} \quad (5)$$

Standard deviation intensity value is used as threshold intensity to binarize the MR image of the brain and is very much helpful for extracting brain portion and differentiating it from to the non-brain portion. MRI of the brain has the significant intensity difference between the background and the foreground, so the use of standard deviation based binarization has been successfully implemented for brain stroke detection purpose.

$$f1(x,y) = \begin{cases} 1 & \text{if } f(x,y) > \sigma \\ 0 & \text{if } f(x,y) \le \sigma \end{cases} \quad (6)$$

The negative transformation is given by the expression

$$s = L - 1 - r \quad (7)$$

For binary image complement, the algorithm use f2(x,y)=1-f1(x,y) which prepare it for the next step of wavelet decomposition. f2(x) can be represented by a scaling function expansion and some number of wavelet function expansions in sub-spaces W_{j_0}, W_{j_0+1}, W_{j_0+2} ….. Thus

$$f2(x) = \sum_k c_{j_0}(k)\varphi_{j_0}(x) + \sum_{j=j_0}^{\infty}\sum_k d_j(k)\psi_{j,k}(x) \quad (8)$$

Here j_0 is an arbitrary starting scale and the $c_{j_0}(k)$, and $d_j(k)$ are relabelled. The $c_{j_0}(k)$ normally defined as approximation or/and scaling coefficients; the $d_j(k)$ are referred to as detail or/and wavelet coefficients. For each higher scale $j \ge j_0$ in the second sum, a finer resolution function a sum of the wavelet is added to the approximation to provide increasing details. If the expansion function forms an orthogonal basis or tight frame, which is often the case, the expansion coefficients are calculated and is shown in the equations below

$$c_{j_0}(k) = \langle f2(x), \varphi_{j_0}(x)\rangle = \int f2(x)\,\varphi_{j_0}(x)\,dx$$

and

$$d_j(k) = \langle f2(x), \psi_{j,k}(x)\rangle = \int f2(x)\,\psi_{j,k}(x)dx \quad (9)$$

Above two coefficients expansion are defined as inner products of a function being expanded and the expansion functions being used where φ_{j_0} and $\psi_{j,k}$ are the expansion functions; c_{j_0} and d_j are the expansion coefficients. Excluding the products that produce 1-D results, like φ(x) ψ(x), the four remaining products create the separable scaling function and separable directionally sensitive wavelets

$$\varphi(x,y) = \varphi(x)\varphi(y) \quad (10)$$

$$\psi^H(x,y) = \psi(x)\psi(y)$$
$$\psi^V(x,y) = \psi(x)\psi(y)$$
$$\psi^D(x,y) = \psi(x)\psi(y) \quad (11)$$

The directional sensitivity is a natural consequence of separability in the above equation (6.11) and it does not increase the computational complexity. The scaled and translated basis functions are.

$$\varphi_{j,m,n}(x,y) = 2^{\frac{j}{2}}\varphi(2^j x - m, 2^j y - n)$$
$$\psi^i{}_{j,m,n}(x,y) = 2^{\frac{j}{2}}\psi^i(2^j x - m, 2^j y - n), \quad i = \{H,V,D\} \quad (12)$$

Here index i identifies the directional wavelets. The discrete wavelet transform of image f2(x, y) is defined by the following equations

$$W_\varphi(j_0,m,n) = \frac{1}{\sqrt{MN}}\sum_{x=0}^{M-1}\sum_{y=0}^{N-1} f2(x,y)\varphi_{j_0,m,n}(x,y)$$
$$W_{\psi^i}(j,m,n) = \frac{1}{\sqrt{MN}}\sum_{x=0}^{M-1}\sum_{y=0}^{N-1} f2(x,y)\psi^i{}_{j,m,n}(x,y), \quad i = \{H,V,D\} \quad (13)$$

As in the 1-D case, j_0 is an arbitrary starting scale and the $W_\varphi(j_0,m,n)$ coefficients define an approximation f2(x, y) at scale j_0. The $W_{\psi^i}(j,m,n)$ coefficients add horizontal, vertical, and diagonal details for scales $j \ge j_0$. normally $j_0=0$ and $N=M=2^J$ so that j=0,1,2,….,J-1 and m=n=0,1,2,….,2^j-1. f2(x, y) is obtained by the inverse discrete transform operations using equations as follows

$$f2(x,y) = \frac{1}{\sqrt{MN}}\sum_m\sum_n W_\varphi(j_0,m,n)\varphi_{j_0,m,n}(x,y) + \frac{1}{\sqrt{MN}}\sum_{i=H,V,D}\sum_{j=j_0}^{\infty}\sum_m\sum_n W_{\psi^i}(j,m,n)\psi^i{}_{j,m,n}(x,y) \quad (14)$$

A point can represent in the plane by a pair (x,y) that stores the x and y Cartesian coordinates for that point.

The equation of the line l through q1 and q2 for coordinates (x1y1) is given by

$$\frac{x - x_1}{x_2 - x_1} = \frac{y - y_1}{y_2 - y_1} \quad (15)$$

Constants a, b, and c can be derived as a = (y_2-y_1); b = -(x_2-x_1); and c = $y_1(x_2- x_1)$ - $x_1(y_2 -y_1)$. A line segment s1 is typically represented by the pair (p,q) of points in the plane that form s1's end points. It is possible to represent a polygon P by a circular sequence of points, called the vertices of P. The segments between consecutive vertices of P are called the edges of P. Polygon P is said to be nonintersecting, or simply if intersections between pairs of edges of P happen only at a common endpoint vertex.
A polygon is convex if it is simple and all its internal angles are less than p. Quick-hull described in [88] is a divide-and-conquer algorithm, similar to quicksort, which divides the problem into two sub-problems and discards some of the points in the given set as interior points, concentrating on remaining points. Quick-hull runs faster than the randomized algorithms because it processes fewer interior points. Also, Quick-hull reuses the memory occupied by old facets. The convex image is now a binary image in which only brain portion is denoted with one, and all non-brain portion contains zero. This convex image is multiplied with the original image, and the resultant image is free of any previously existing artifacts, noise, and skull as such removals are critical for brain abnormality detection.

To segment and detect abnormalities the power-law transformations is applied on f3 image in basic form of

$$f4(x,y) = c * f3(x,y)^{\gamma} \quad (16)$$

Where c and γ are the positive constant and the above equation is sometimes written as

$$f4(x,y) = c * (f3(x,y) + \varepsilon)^{\gamma} \quad (17)$$

ε is used to report for a measurable output when the input is zero. However, offsets are an issue of display calibration, and as a result, they are ignored. Transform values of γ>1 have accurately the opposite effect as those generated with principle values of γ <1 and to the identity transformation when c= γ =1. Gamma correction is significant for displaying an image appropriately on a computer screen, and particular care must be taken to reproduce colors accurately. This requires knowledge of gamma correction as any change in the value of gamma will not only alter the brightness but also the corresponding red, green and blue ratios. By setting γ =3, and c=1 in gamma transformation abnormal portion become more prominently projected. The total intensity, by the sum of the average and standard deviation of the Gamma transformed image, is finally selected. Thus the final selection is given by

$$T = \frac{1}{MN}\sum_{x=0}^{M-1}\sum_{y=0}^{N-1} f4(x,y) + \sqrt{\frac{1}{MN}\sum_{x=0}^{M-1}\sum_{y=0}^{N-1}(f4(x,y) - \mu)^2} \quad (18)$$

Abnormal lesions are selected from the final intensity T which is in the form of binary output and is stored in f5(x, y).

$$f5(x,y) = \begin{cases} 0 & f4(x,y) \le T \\ 1 & f4(x,y) > T \end{cases} \quad (19)$$

f5 is the binarized results which consist of abnormal lesions along with some normal tissues for T2 and PD type MR brain images. Figure 1 shows the output.

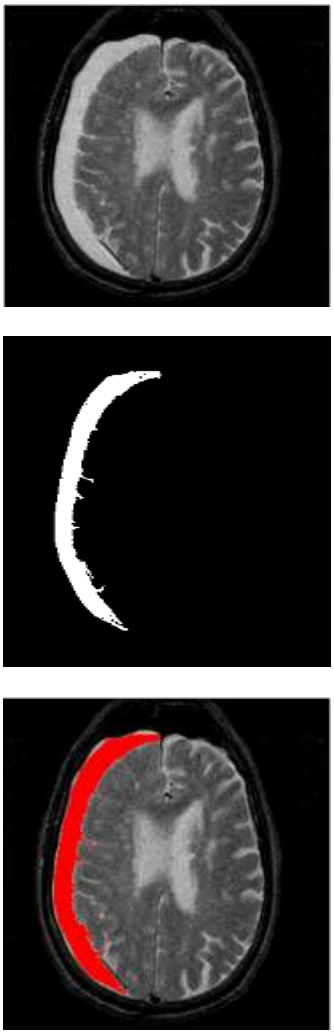

Figure. 1. Segmented part Marked with Red.

CONCLUSIONS

A large number of approaches have been proposed by various researchers to deal with MRI images. The development of automatic and accurate CAD in characterizing brain lesions are essential and it remains an open problem. Lesion detection, segmentation or separation of a particular region of interest is an important process for diagnosis. Computer aided surgery also requires previous analysis of lesion area inside the

brain. This process is a challenging process due to the complexity and large variations in the anatomical structures of human brain tissues, the variety of the possible shapes, locations and intensities of various types of lesions. Many methods need some preprocessing technique for improvement of accurate identification of brain abnormalities. In the threshold intensity based binarized segmentation; Kapur method can provide better results than other for brain abnormalities segmentation. But Kapur thresholding suffers from under segmentation and spurious lesion generations for many brain images. Most of the binarized fail due to large intensity difference of foreground and background i.e. the black background of MRI image. In region growing methodologies are not standard methods for validating segmentation; the main problem is the quality of segmentation in the border of the tumor. These methods are suitable for the homogeneous tumor but not for heterogeneous tumor. Classification based segmentation can segment tumor accurately and produce good results for large data set, but undesirable behaviors can occur in a case where a class is under-represented in training data. Clustered based segmentation performs very simple, fast and produces good results for the non-noise image but for noise images, it leads to serious inaccuracy in the segmentation. In a neural network-based segmentation perform little better on noise field and no need of assumption of any original data allocation, but the learning process is one of the great disadvantages of it. In spite of several difficulties, an atomization of brain tumor segmentation using a combination of a threshold based, preprocessing and the level set can overcome the problems and gives efficient and accurate results for brain abnormality detection. Accurate detection is the basis for calculating important features of brain lesion such as size, classification, heterogeneity, and volume of the lesions.

REFERENCES

1. A. Arber, S. Faithfull, M. Plaskota, C. Lucas, and K. de Vries, “A study of patients with a primary malignant brain tumour and their carers: symptoms and access to services,” Int. J. Palliat. Nurs, Feb. 2010; 16(1): 24–30.
2. L. Landini, V. Positano, and M. F. Santarelli, Advanced image processing in magnetic resonance imaging. CRC/Taylor & Francis, 2005.
3. A. Işın, C. Direkoğlu, and M. Şah, “Review of MRI-based Brain Tumor Image Segmentation Using Deep Learning Methods,” Procedia Comput. Sci., Jan. 2016; 102: 317–324.
4. X. Liu, M. Niethammer, R. Kwitt, N. Singh, M. McCormick, and S. Aylward, “Low-Rank Atlas Image Analyses in the Presence of Pathologies,” IEEE Trans. Med. Imaging, Dec. 2015; 34(12): 2583–2591.
5. D. J. Hemanth, A. Aber, and M. M. al-Rifaie, “Deploying swarm intelligence in medical imaging identifying metastasis, micro-calcifications and brain image segmentation,” IET Syst. Biol., Dec. 2015; 9(6): 234–244.
6. V. Anitha and S. Murugavalli, “Brain tumour classification using two-tier classifier with adaptive segmentation technique,” IET Comput. Vis., Feb. 2016; 10(1): 9–17.
7. A. Islam, S. M. S. Reza, and K. M. Iftekharuddin, “Multifractal Texture Estimation for Detection and Segmentation of Brain Tumors,” IEEE Trans. Biomed. Eng., 2013; 60(11).
8. M. C. Clark, L. O. Hall, D. B. Goldgof, R. Velthuizen, F. R. Murtagh, and M. S. Silbiger, “Automatic tumor segmentation using knowledge-based techniques,” IEEE Trans. Med. Imaging, , Apr. 1998; 17(2): 187–201.
9. M. Huang, W. Yang, Y. Wu, J. Jiang, W. Chen, and Q. Feng, “Brain Tumor Segmentation Based on Local Independent Projection-Based Classification,” IEEE Trans. Biomed. Eng., Oct. 2014; 61(10): 2633–2645.
10. B. H. Menze, K. Van Leemput, D. Lashkari, T. Riklin-Raviv, E. Geremia, E. Alberts, P. Gruber, S. Wegener, M.-A. Weber, G. Szekely, N. Ayache, and P. Golland, “A Generative Probabilistic Model and Discriminative Extensions for Brain Lesion Segmentation— With Application to Tumor and Stroke,” IEEE Trans. Med. Imaging, Apr. 2016; 35(4): 933–946.
11. E. Ilunga–Mbuyamba, J. G. Avina–Cervantes, J. Cepeda–Negrete, M. A. Ibarra–Manzano, and C. Chalopin, “Automatic selection of localized region-based active contour models using image content analysis applied to brain tumor segmentation,” Comput. Biol. Med., Dec. 2017; 91: 69-79.
12. S. Charutha and M. J. Jayashree, “An efficient brain tumor detection by integrating modified texture based region growing and cellular automata edge detection,” 2014 Int. Conf. Control. Instrumentation, Commun. Comput. Technol. ICCICCT, 2014; 1193–1199.